

PAPER

Effects of bio-inspired infill design on the mechanical properties of ultrasonic vibration assisted 3D printed samples

To cite this article: Thavinnesh Kumar Rajendran *et al* 2024 *Eng. Res. Express* **6** 025430

View the [article online](#) for updates and enhancements.

You may also like

- [Elephant trunk wrinkles: a mathematical model of function and form](#)
Yang Liu, Alain Goriely and L Angela Mihai
- [Mechanical properties comparison of PLA, tough PLA and PC 3D printed materials with infill structure – Influence of infill pattern on tensile mechanical properties](#)
Adi Pandzic and Damir Hodzic
- [Mechanical Properties of 3D Printed Polylactic Acid Product for Various Infill Design Parameters: A Review](#)
T J Suteja and A Soesanti

Engineering Research Express



PAPER

Effects of bio-inspired infill design on the mechanical properties of ultrasonic vibration assisted 3D printed samples

RECEIVED
9 March 2024

REVISED
23 May 2024

ACCEPTED FOR PUBLICATION
29 May 2024

PUBLISHED
13 June 2024

Thavinnesh Kumar Rajendran , Mohd Afiq Shahrum, Shajahan Maidin and Shafinaz Ismail

Faculty of Industrial & Manufacturing Technology & Engineering, Universiti Teknikal Malaysia Melaka, Hang Tuah Jaya, 76100 Durian Tunggal, Melaka, Malaysia

E-mail: shajahan@utem.edu.my

Keywords: additive manufacturing, fused deposition modeling, ABS, PLA, bio-inspired infill design

Abstract

This paper study the tensile strength and microstructure of the 3D bio-inspired printed samples by comparing the ultrasonic vibration assisted test samples with standard ABS and PLA samples with three different bio-inspired infill designs namely elephant trunk, bamboo and leaf. The test samples were printed with optimal printing process parameters and 0 kHz and 20 kHz frequency of ultrasonic vibration. SolidWorks software was used to design the bio-inspired infill designs and create the 3D-printed test samples. Tests to evaluate mechanical properties and microstructure were carried out after printing the test samples. The investigation primarily focuses on the impact of ultrasonic vibration assisted 3D bio-inspired printed samples of ABS and PLA materials. This research explores using ultrasonic vibration assistance to enhance the tensile strength of 3D-printed infills. The elephant trunk inspired infill design with ABS at 20 kHz achieved the best results, suggesting that ultrasonic vibration strengthens intermolecular bonding. The bamboo inspired infill performed poorly due to its design, while PLA deformed due to lower heat resistance. Overall, ultrasonic frequency improved layer bonding, especially for the elephant trunk infill, indicating potential for further optimization. These results demonstrate the effectiveness of bio-inspired infill solutions, mainly the ABS elephant trunks with ultrasonic 20 kHz of vibration.

Nomenclature

AM	Additive Manufacturing
FDM	Fused Deposition Modelling
CAD	Computer-Aided Design
PLA	Poly-Lactic Acid
ABS	Acrylonitrile Butadiene Styrene

1. Introduction

Additive manufacturing (AM), often referred to as 3D printing, is a revolutionary technology that constructs objects layer by layer using materials. This method provides several advantages over traditional manufacturing, including greater design flexibility, cost-efficiency, and improved productivity. Since its introduction in the 1980s, additive manufacturing has rapidly evolved, transforming various industries and offering innovative engineering solutions [1]. AM has garnered significant interest from academia and industry alike, thanks to its unique capabilities such as tool-less production, the ability to create complex shapes, and efficient use of resources.

Manufacturing processes are broadly categorized into subtractive, formative, and additive [2, 3]. Prototypes have been generated using a combination of additive and subtractive manufacturing techniques [4]. AM is the

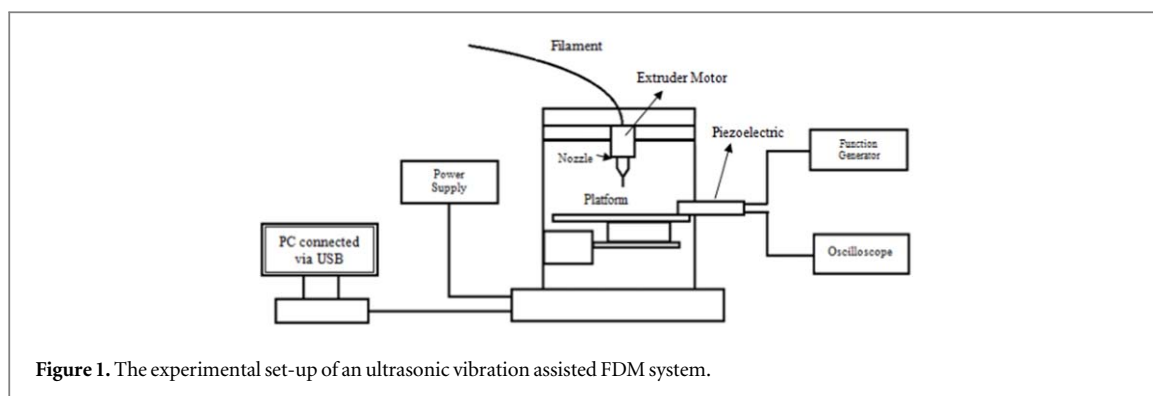


Figure 1. The experimental set-up of an ultrasonic vibration assisted FDM system.

process of fabricating items from 3D model data, usually layer by layer, as defined by the American Society for Testing and Materials (ASTM) [5, 6]. Historically used for prototyping, AM creates solid objects directly from a device without needing any equipment. Parts are built layer by layer using thin powder-form materials, contrasting with traditional machining methods [7].

AM is a relatively recent method compared to traditional manufacturing processes [8]. This technology allows manufacturers to rethink product design and production processes completely. Using Computer-Aided Design (CAD), AM adds materials to create parts instead of subtracting them, as in traditional methods. This innovative design-driven approach offers advantages such as reduced material usage, shorter production times, and optimized manufacturing for improved product performance. Additionally, AM can apply coatings to components to prevent corrosion and wear, and it can combine layers of different materials to create complex three-dimensional structures under computer control, also known as Solid Freedom Manufacturing or SFF [9–11].

Although AM has garnered significant attention, several challenges must be addressed to enhance its efficacy in industrial production. AM of metallic parts involves intricate processes and numerous process parameters. The layer-by-layer construction technique leads to material solidification and heat cycling during manufacturing, creating complex thermal conditions that induce phase transitions from liquid to solid and within the solid state. Post-treatment methods like hot isostatic pressing (HIP) and heat treatment further alter the material. These material changes significantly impact the component's performance, making it challenging to achieve the desired performance and quality using AM [12, 13].

AM technologies necessitate adaptable specialists eager to use manufacturing technologies, especially in terms of innovation and advancement [14]. Thermoplastics were initially utilized to create AM, which has since expanded to include processes for almost all plastics, biomaterials, ceramics, metals, electronics, and composite materials [15].

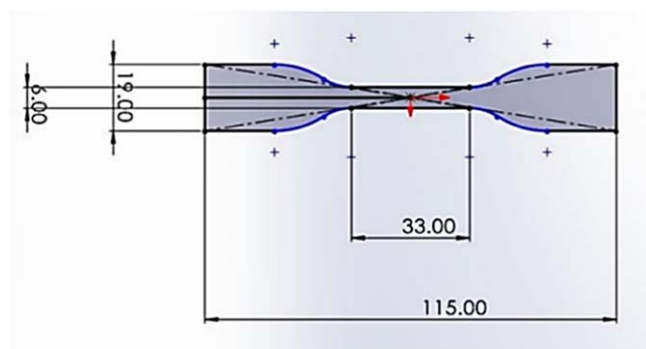
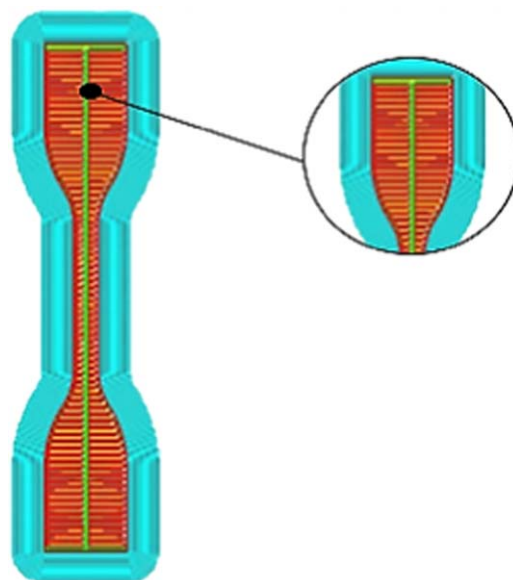
The thermoplastic polymer matrix plays a crucial role in Fused Deposition Modeling (FDM) fiber-reinforced composites. Acrylonitrile Butadiene Styrene Polymer (ABS) and Polylactic Acid Polymer (PLA) are commonly used materials in this process due to their low melting temperatures, which make them compatible with FDM. However, the inherent limitations in strength and functional properties of pure polymer printed parts restrict their use primarily to building conceptual or prototype samples [16]. ABS is often used in manufacturing toys and household items due to its relatively low harmful effects on humans compared to other polymer materials. Its superior heat, chemical, and moisture resistance make it a preferred choice for developing testing samples [17]. While ABS demonstrate better impact strength than PLA, PLA exhibits higher tensile strength [18, 19].

Wickramasinghe *et al* (2020) [20] reviewed the influence of defects on the mechanical performance of fiber-reinforced composites, examining the impact of printing parameters like layer thickness, infill pattern, raster angle, and fiber orientation. The primary goal of this project is to explore the implementation of bio-inspired infill design patterns for printing FDM samples with the desired strength using ABS and PLA materials. Tensile and microstructure tests will be conducted to compare ABS and PLA materials. ABS and PLA filaments will be used to fabricate the test samples, which will then be compared with standard ABS and PLA samples to assess the effectiveness of the ultrasonic-assisted printing process.

Infill design is a critical element in the FDM process. It is the method of printing the interior design of a printed component. Many different filling patterns exist, including hexagonal, linear, and diamond shapes [21]. Nature offers abundant inspiration, both visually and functionally. Terms like 'bionic,' 'bio-inspired,' and 'biomimicry' describe mimicking nature's shapes or functions. Biomimetics, rooted in Greek origins, involves imitating natural processes to solve human problems. Nature has perfected organic structure–function relationships with unique properties. Biomimetics facilitates interdisciplinary collaboration and technology

Table 1. Dimension of the test samples.

	Length	Width	Thickness
Dimension	115.0 mm	19.0 mm	3.3 mm

**Figure 2.** Design of test sample.**Figure 3.** Elephant trunk inspired pattern.

transfer to industries seeking sustainable solutions. Many biomimetic principles find application due to their practicality and effectiveness. For example, bio-inspired tree branch joints are used in aircraft engineering to enhance the damage tolerance of composite hulls. Multi-corner tubes inspired by bamboo and honeycomb shapes strengthen materials without adding weight. Biomimetic designs promise functional integration, weight reduction, and simplified complexity [22].

2. Methodology

2.1. Experimental setup and sample design

Figure 1 shows the experimental set-up for the ultrasonic vibration assisted FDM using Ender 6, where the ultrasonic piezoelectric transducer is clamped horizontally on the surface of the platform. The piezoelectric is clamped on the side of the platform; thus, only the platform will be vibrated by the piezoelectric. The piezoelectric must be correctly placed on the platform to prevent the nozzle from touching each other and moving up and down smoothly on the built platform. The vibration was transmitted directly to the platform, while the sample received vibration with a specific frequency during printing.

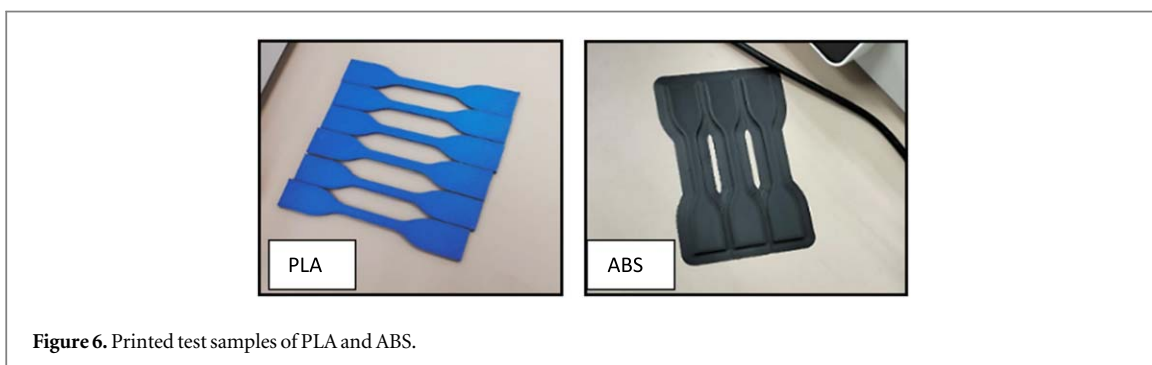
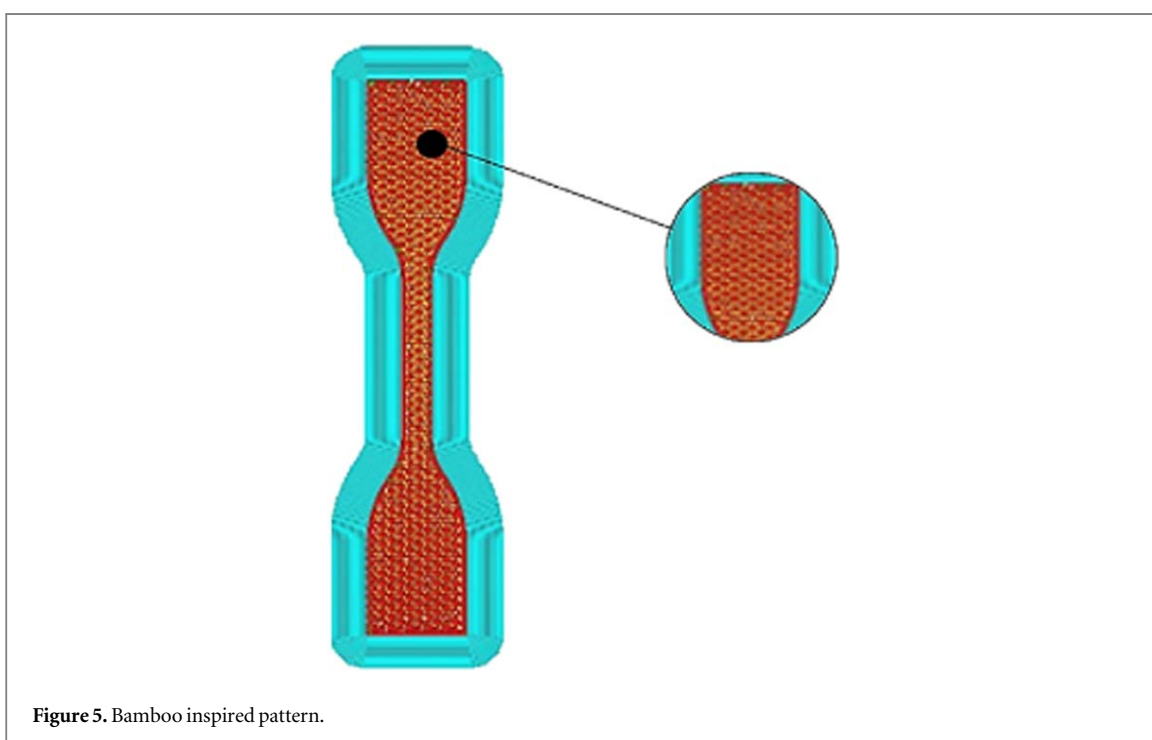
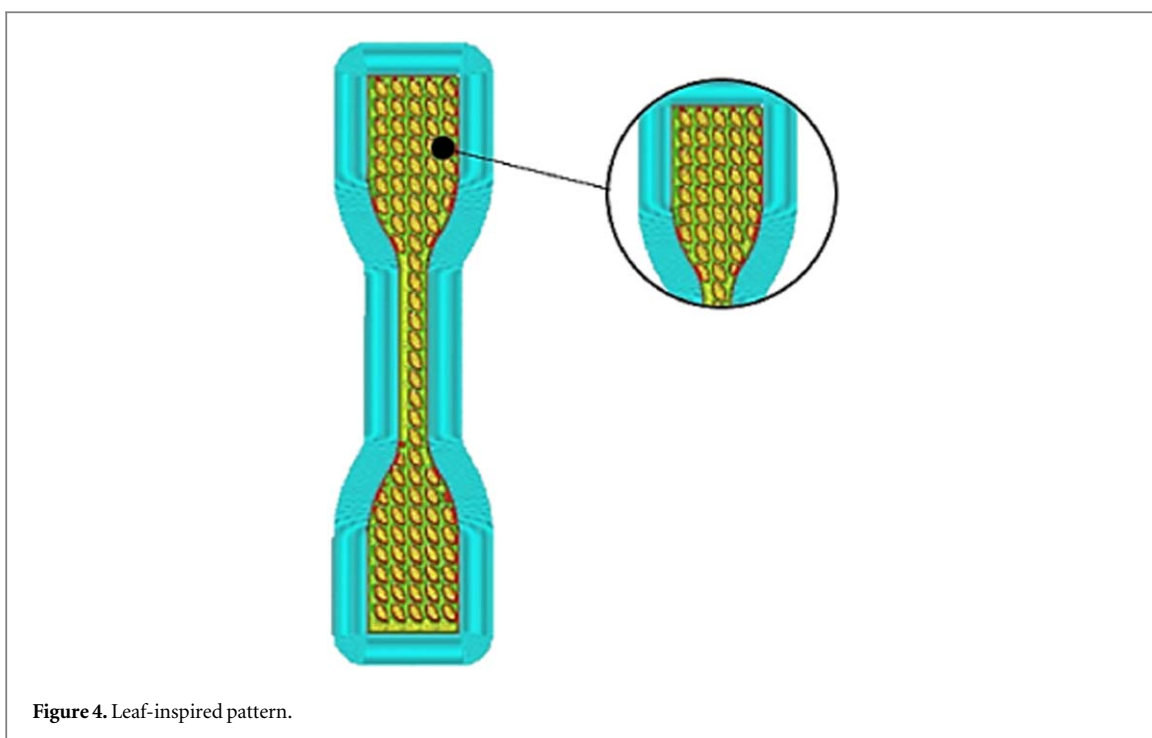


Table 2. Equipment used for 3D printing.

Instrument	Model
3D Printer	Ender 6
Ultrasonic vibration generator	BK precision 4052
Transducer	Piezoelectric transducer
Frequency setting	0 & 20 kHz

Table 3. Parameters of printed sample (Maidin *et al* 2022).

Type of filament	Generic ABS/ PLA
Print profile	0.15 mm
Layer height	0.2 mm
Infill density	0.0%
Printing temperature	245.0 °C
Build plate temperature	85.0 °C
Print speed	60.0 mm s ⁻¹
Build plate adhesion type	Brim

Table 4. The specification of the piezoelectric transducer.

Specification of piezoelectric transducer	INC (Piezo System)
Type	Standard quick-mount extension actuator
Weight	2.3 g
Max voltage	±90 V
Deflection	3.6 µm
Max amplitude	10 µm

Table 1 and figure 2 illustrate the experimental dimensions of the dog bone samples. The SolidWorks software was employed to design the test samples using three specific infill designs. Samples were printed according to ASTM Standard Type IV.

Three distinct infill designs were developed, each inspired by natural elements such as bamboo, leaves, and elephant trunks. The intricate patterns of these elements were meticulously designed using SolidWorks, as showcased in figures 3, 4, and 5 below. These figures provide a detailed visual representation of how the designs were created following the specifications outlined in the Type IV ASTM Standard. Overall, these natural elements likely offered a combination of strength, flexibility, and aesthetic appeal that are ideal for infill designs.

2.2. Printing parameters

Figure 6 shows the printed test samples of PLA and ABS. A total of thirty-six samples were printed. Eighteen test samples for PLA and eighteen for ABS material are printed. The ultrasonic vibration with two different frequencies is needed for 3D printing, which is 0 kHz and 20 kHz. Table 2 states the equipment used for the printing process.

FDM technology is distinguished by its use of specialized 3D printers and industrial-grade thermoplastics, resulting in unprecedented accuracy in component creation. Table 3 presents the recommended parameters for ABS and PLA filament. The parameters were chosen due to their relevance to the research objectives and consistent mention in the existing literature [23], highlighting their significance in similar studies. In this study, a specified ideal parameter was established before initiating the printing process. In this scenario, the infill percentage was not optimized and was instead set to 0% due to the creation of the infill designs.

2.3. Piezoelectric transducer

The piezoelectric transducer is an exceptional device for converting high-frequency electrical energy into mechanical vibrations. This study assumes the role of generating longitudinal vibrations, particularly at a max frequency of 20 kHz. In the scope of this study, two specific frequencies, specifically 0 kHz, and 20 kHz, have been selected.



Figure 7. Tensile test sample in universal tensile machine.

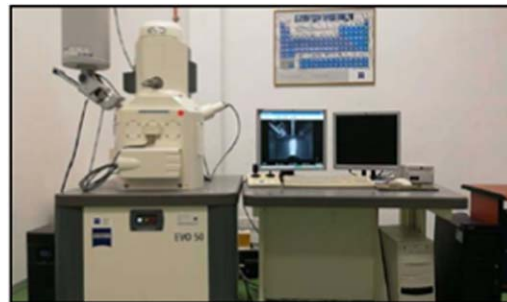


Figure 8. Carl Zeiss Evo 50 SEM machine.

The precise design of this system is notable for its effectiveness, where the ultrasonic piezoelectric transducer is clamped horizontally on the surface of the platform. The piezoelectric is clamped on the side of the platform; thus, only the platform will be vibrated by the piezoelectric. The piezoelectric will need to be placed appropriately on the platform to prevent the nozzle from touching each other and for it to move up and down on the built platform smoothly. The vibration was transmitted directly to the platform, while the sample received vibration with a specific frequency during printing. For a deeper dive into the technical aspects, table 4 offers a detailed summary of the piezoelectric transducer's specifications.

2.4. Tensile test

The destructive test technique known as tensile testing provides information regarding metallic materials' tensile strength, yield strength, and flexibility. It measures how much a composite or plastic sample stretches or elongates before breaking and the force required to fracture it. The material's tensile strength is ascertained by applying a pulling force to both ends of the samples and stretching them together in the opposite direction. The test was stopped when the samples broke, and the material's tensile strength was discovered [24]. Figure 7 depicts the clamping of the tensile sample on both sides to initiate the tensile test.

2.5. Microstructure analysis

Scanning Electron Microscope (SEM) is a machine that provides nanoscale-level information on various materials without requiring sample preparation. SEM machine generates the images by scanning a focused

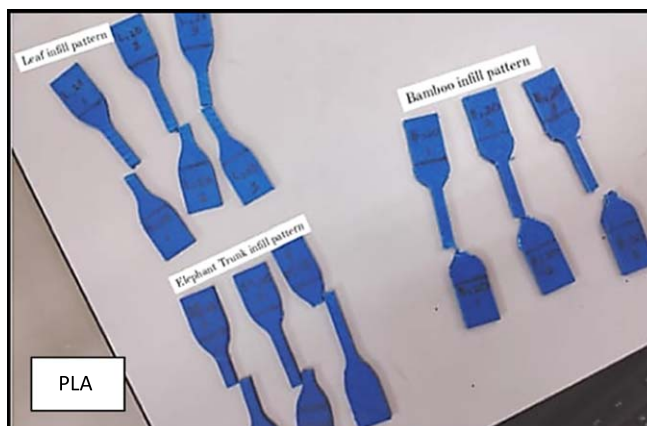


Figure 9. Tensile test samples for PLA.

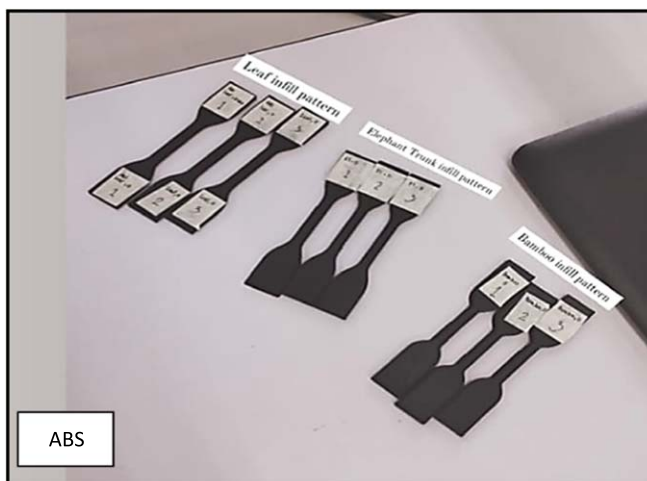


Figure 10. Tensile test samples for ABS.

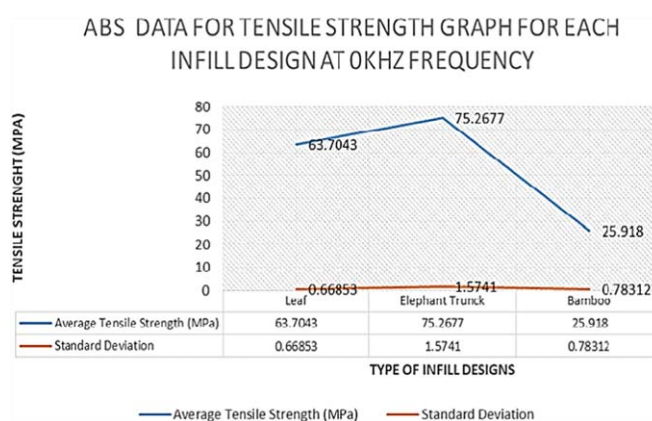
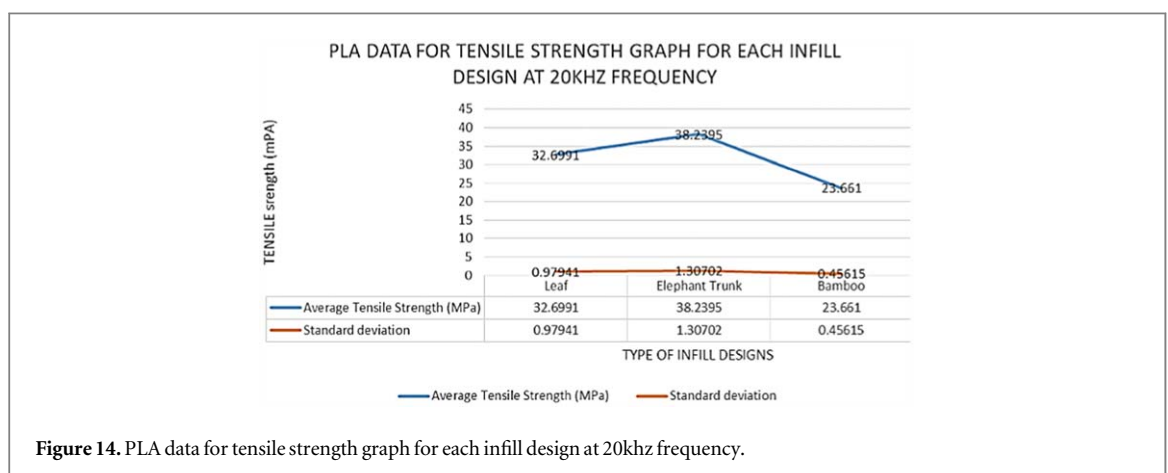
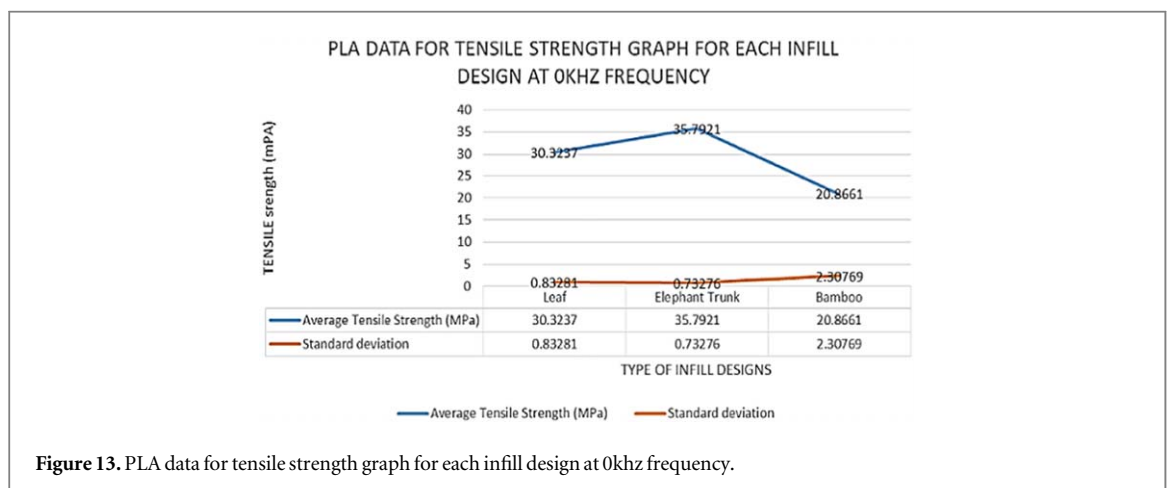
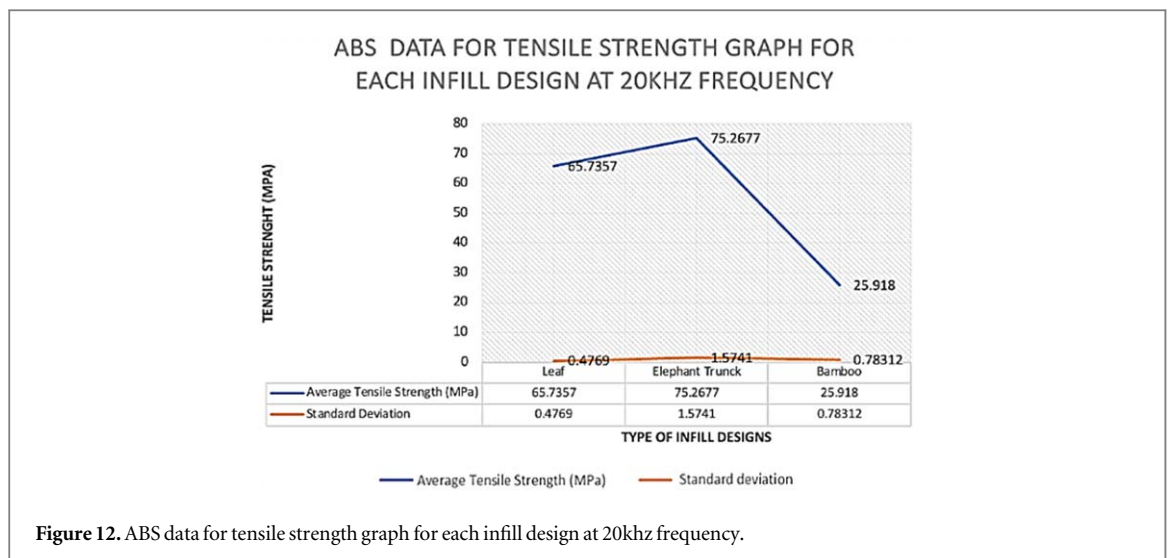


Figure 11. ABS data for tensile strength graph for each infill design at 0 kHz frequency.

electron beam across a surface. The beam electrons will connect with the samples and produce a different signal that may be used to discover its surface topography and composition. Figure 8 shows the Carl Zeiss Evo 50 SEM machine used in this study to examine the porosity on the surface structure of the ABS and PLA samples.

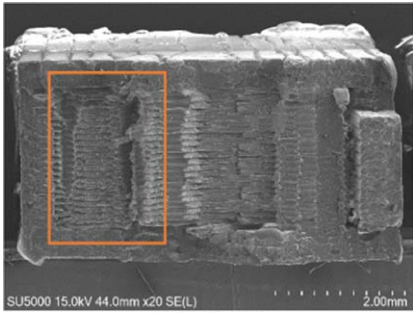
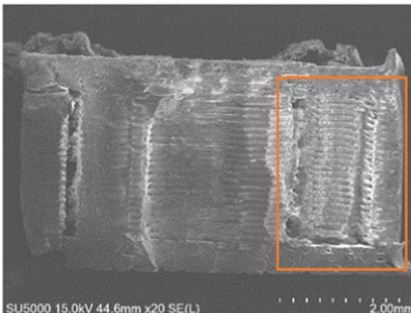
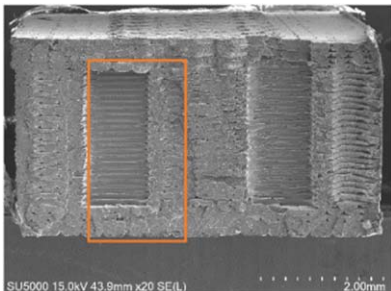
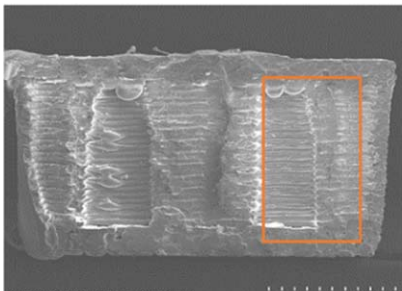
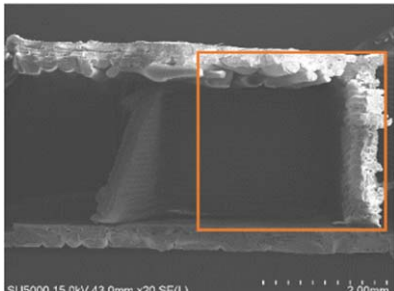
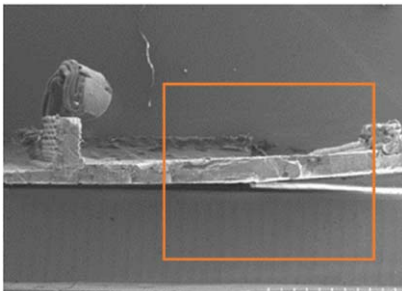


3. Results and discussion

3.1. Tensile test

The tensile test was conducted thirty-six times for two types of material, ABS and PLA material. The tensile test was conducted to observe the material behaviour on tensional loading. By doing the tensile test, material properties such as tensile strength, yield strength, and stress failure of ABS and PLA can be determined. By using this measurement, the material's stiffness can also be determined, which is known as the modulus of elasticity. The sample's condition before and after the test is shown in figures 9 and 10.

Table 5. Scanning electron microscopy image of ABS.

Scanning electron microscopy (SEM) Image for ABS of each infill design	
	
LEAF,0KHZ	LEAF,20KHZ
	
ELEPHANT TRUNK, 0KHZ	ELEPHANT TRUNK, 20KHZ
	
BAMBOO, 0KHZ	BAMBOO, 20KHZ

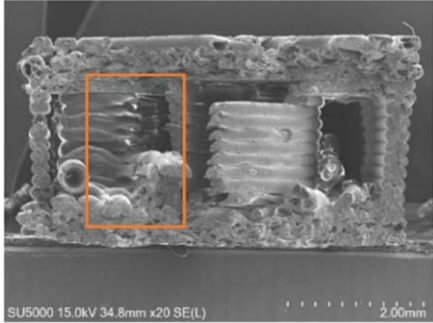
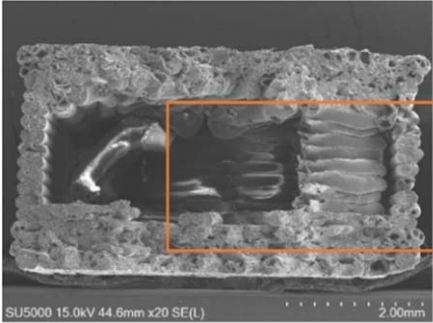
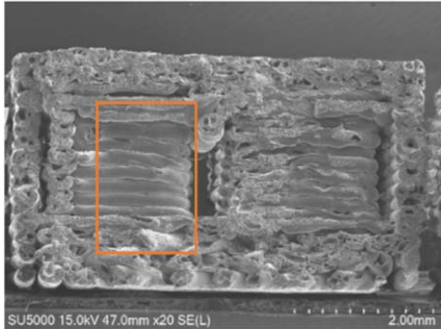
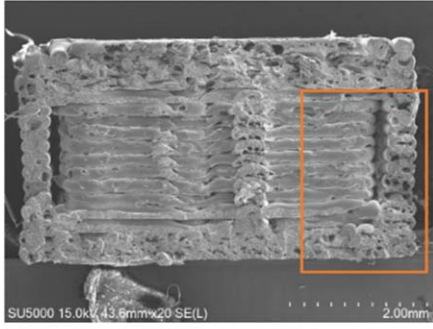
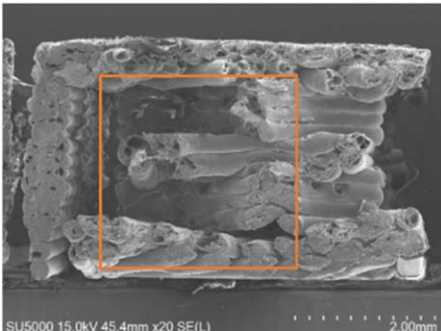
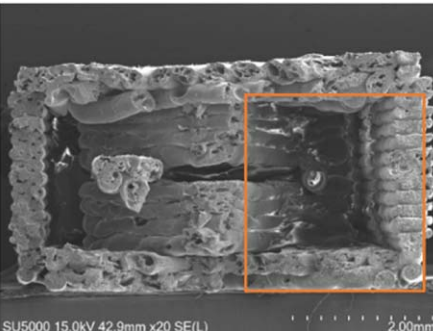
3.2. Comparison of tensile test of ABS using different infill designs

The results in this study are gathered in terms of the graph and calculated based on the test sample's infill pattern, which is divided into two frequency categories: 20 kHz and 0 kHz. Figures 11 and 12 below show tensile strength values for the test samples at 0 kHz and 20 kHz for PLA and ABS material.

As stated in figure 11, at 75.2677 MPa, the Elephant Trunk has the highest average tensile strength. The leaf has the second-highest strength, with an average tensile strength of 63.7043 MPa. At 25.918 MPa, bamboo has the lowest average tensile strength. For every infill design, the standard deviation is additionally displayed. The standard deviation indicates the degree to which the data deviates from the average. A smaller standard deviation indicates a closer clustering of the data around the average, while a higher standard deviation indicates a more dispersed data set. Elephant Trunk, with 0.66853 MPa, has the lowest standard deviation. This demonstrates that Elephant Trunk's data is the most closely grouped around the mean. At 1.5741 MPa, Leaf has the second-lowest standard deviation. With a standard deviation of 0.78312 MPa, bamboo has the highest value. This indicates that bamboo has the most dispersed data.

Figure 12 shows that the elephant Trunk, with 75.2677 MPa, has the highest average tensile strength. The leaf has the second-highest value, with an average tensile strength of 65.7357 MPa. At 25.918 MPa, bamboo has the lowest average tensile strength. Elephant Trunk, at 0.4769 MPa, has the lowest standard deviation. This indicates that Elephant Trunk's data is the most closely grouped around the mean. At 1.5741 MPa, Leaf has the second-

Table 6. Scanning electron microscopy image of PLA.

Scanning electron microscopy (SEM) image for PLA of each infill design	
	
LEAF,0KHZ	LEAF,20KHZ
	
ELEPHANT TRUNK, 0KHZ	ELEPHANT TRUNK, 20KHZ
	
BAMBOO, 0KHZ	BAMBOO, 20KHZ

lowest standard deviation. With a standard deviation of 0.78312 MPa, bamboo has the highest value. This indicates that bamboo has the most dispersed data. Based on the statistics, the elephant trunk is the most effective infill design overall, with leaf and bamboo coming in second and third. Elephant Trunk is the most dependable infill design since its data shows the slightest variance.

3.3. Comparison of tensile test of PLA using different infill designs

Figure 13 shows that Elephant Trunk, with 35.7921 MPa, has the highest average tensile strength. The leaf has the second-highest strength, with an average tensile strength of 30.3237 MPa. At 20.8661 MPa, bamboo has the lowest average tensile strength. Elephant Trunk, at 0.83281 MPa, has the lowest standard deviation. At 0.73276 MPa, Leaf has the second-lowest standard deviation. With a standard deviation of 2.30769 MPa, bamboo has the highest value.

Figure 14 displays the average tensile strength of the leaf, elephant trunk, and bamboo for each infill design at a frequency of 20 kHz. Elephant Trunk, with 38.2395 Mpa, has the highest average tensile strength. The leaf has the second-highest strength, with an average tensile strength of 32.6991 Mpa. At 23.661 Mpa, bamboo has the

lowest average tensile strength. Elephant Trunk, at 0.97941 Mpa, has the lowest standard deviation. At 1.30702 Mpa, Leaf has the second-lowest standard deviation. With a standard deviation of 0.45615 Mpa, bamboo has the highest value.

3.4. Scanning electron microscopy

Tables 5 and 6 compare all three infill designs at frequencies of 0 kHz and 20 kHz for both ABS and PLA materials. The marked area showed how the structure looks inside every infill design. Various factors affected the microstructure of each sample, such as material, infill design, frequencies, and errors in the testing machine. Elephant trunk, 20 kHz, has good layer bonding. Ultrasonic vibration can enhance the bonding between the individual layers of the printed object. The vibrations help to increase the intermolecular forces between the layers, resulting in stronger adhesion and improved overall structural integrity [25]. Due to the gap between the layers, no layer bonding is created for the bamboo design. Table 6 shows that PLA has a lower heat resistance, which causes the deformation inside the infill patterns due to lower temperatures. With a 20 kHz frequency, the elephant trunk pattern still has good layer bonding compared to the bamboo pattern.

4. Conclusion

This work effectively met the goal of developing and accessing bio-inspired infill designs for tensile strength with ultrasonic support. At ultrasonic frequencies of 0 kHz and 20 kHz, the study compared three infill designs (elephant trunk, leaf, and bamboo) with conventional ABS and PLA materials. Elephant trunk infill in ABS material showed the best layer bonding, especially at 20 kHz, proving that ultrasonic vibration helps increase adhesion and intermolecular forces. Compared to other designs and frequencies, it attained a higher tensile strength. Elephant trunk design is much more successful than leaf infill design, although bamboo is less effective. The bamboo infill pattern exhibited poor layer bonding due to its design featuring holes, rendering it unsuitable for tensile applications. This finding aligns with a study by [26], where an infill design with holes also showed inadequate layer bonding. Because PLA has lesser heat resistance, it deformed inside the infill patterns, highlighting the significance of material selection. In general, layer bonding was enhanced by ultrasonic frequency (20 kHz), particularly for the elephant trunk design, indicating the possibility for additional optimization.

This study shows that bio-inspired infill designs, especially elephant trunks with ultrasonic support at 20 kHz, can outperform conventional materials in tensile strength. It is advised that more studies be conducted on various bio-inspired designs, materials, and ultrasonic parameters to broaden this intriguing 3D printing component optimization strategy. Consider measuring the noted increases in tensile strength and bonding for more robust findings. Examine how ultrasonic vibration affects material characteristics and structural integrity over the long run. Future research can build on this foundation and further enhance the construction of high-performance 3D-printed structures using ultrasonic vibration and bio-inspired infill designs by addressing these issues.

Acknowledgments

This work was supported by the Universiti Teknikal Malaysia Melaka (UTeM) and the Ministry of Higher Education Malaysia for awarding the Zamalah Scholarship (Skim Zamalah UTeM).

Data availability statement

All data that support the findings of this study are included within the article (and any supplementary files).

ORCID iDs

Thavinnesh Kumar Rajendran  <https://orcid.org/0000-0002-9397-0174>

Shafinaz Ismail  <https://orcid.org/0000-0001-7883-250X>

References

- [1] Saleh Alghamdi S, John S, Roy Choudhury N and Dutta N K 2021 Additive manufacturing of polymer materials: progress, promise and challenges *Polymers* **13** 753

- [2] Zivanovic S T, Popovic M D, Vorkapic N M, Pjevic M D and Slavkovic N R 2020 An overview of rapid prototyping technologies using subtractive, additive and formative processes *FME Transactions* **48** 246–53
- [3] Paolini A, Kollmannsberger S and Rank E 2019 Additive manufacturing in construction: a review on processes, applications, and digital planning methods *Addit Manuf* **30** 100894
- [4] Abdulhameed O, Al-Ahmari A, Ameen W and Mian S H 2019 Additive manufacturing: challenges, trends, and applications *Advances in Mechanical Engineering* **11** (2) 1–27
- [5] Pérez M L, Carou D, Rubio E and Teti R 2020 Current advances in additive manufacturing *Procedia CIRP* **88** 439–44
- [6] Srinivasulu Reddy K and Dufera S 2016 Additive manufacturing technologies *Best: International Journal of Management, Information Technology and Engineering (BEST: IJMITE)* **4** 89–112
- [7] Ma Q, Rejab M R M, Kumar A P, Fu H, Kumar N M and Tang J 2020 Effect of infill pattern, density and material type of 3D printed cubic structure under quasi-static loading *Proc. Inst. Mech. Eng. Part C J. Mech. Eng. Sci.* **235** 4254–72
- [8] Aiman Sukindar N et al 2022 A review study on the effect of printing parameters of fused deposition modelling (FDM) metal polymer composite parts on mechanical properties and surface roughness *Nor Aiman et al. Malaysian Journal of Microscopy* **18** 281–97
- [9] Karar G C, Kumar R and Chattopadhyaya S 2021 An analysis on the advanced research in additive manufacturing *Lecture Notes in Mechanical Engineering* (Springer Science and Business Media Deutschland GmbH) 229–77
- [10] Pandey K, Misra R, Patowari P and Dixit U 2021 *Recent Advances in Mechanical Engineering: Select Proceedings of ICRAE 2020* (Springer)
- [11] Moylan S, Slotwinski J A, Cooke A L, Jurrens K K and Donmez M A 2012 *Proposal for a Standardized Test Artifact for Additive Manufacturing Machines and Processes* (National Institute of Standards and Technology)
- [12] Shahrubudin N, Lee T and Ramlan R 2019 An overview on 3D printing technology: technological, materials, and applications *Procedia Manufacturing* **35** 1286–96
- [13] DebRoy T, Wei H L, Zuback J S, Mukherjee T, Elmer J W, Milewski J O and Zhang W 2018 Additive manufacturing of metallic components—process, structure and properties. *Progress in Materials Science* **92** 112–224
- [14] Jiménez M, Romero L, Domínguez I A, Espinosa M D M and Domínguez M 2019 Additive manufacturing technologies: an overview about 3D printing methods and future prospects *Complexity* **2019** 1–309656938
- [15] Guessasma S, Belhabib S and Nouri H 2019 Microstructure, thermal and mechanical behavior of 3D printed acrylonitrile styrene acrylate *Macromol. Mater. Eng.* **304** 1–20
- [16] Maidin S, Hayati N M N, Rajendran T K and Muhammad A H 2023 Comparative analysis of acrylonitrile butadiene styrene and polylactic acid samples' mechanical properties printed in vacuum *Additive Manufacturing* **67** 103485
- [17] Novakova-Marcincinova L and Novak-Marcincin J 2013 Verification of mechanical properties of ABS materials used in FDM rapid prototyping technology *Proceedings in Manufacturing Systems* **8** 87–92 http://www.icmas.eu/Journal_archive_files/Vol_8-Issue2-2013-PDF/87-92_Marcincin.pdf
- [18] Vinyas M, Athul S J, Harusampath D and Nguyen Thoi T 2019 Mechanical characterization of the Polylactic acid (PLA) composites prepared through the Fused Deposition Modelling process *Mater. Res. Express* **6** (10) 105359
- [19] Cantrell J T et al 2017 Experimental characterization of the mechanical properties of 3D-printed ABS and polycarbonate parts *Rapid Prototyping Journal* **23** 811–24
- [20] Wickramasinghe S, Do T and Tran P 2020 FDM-Based 3D printing of polymer and associated composite: a review on mechanical properties, defects, and treatments *Polymers* **12** MDPI AG 1–42
- [21] Qavi A and Rahim M R U 2022a A Review on Effect of Process Parameters On FDM-Based 3D Printed PLA Materials (ResearchGate) https://researchgate.net/publication/361797550_A_Review_On_Effect_Of_Process_Parameters_On_FdmBased_3d_Printed_Pla_Materials/citations
- [22] Raheem A A, Hameed P, Whenish R, Elsen R S, Aswin G, Jaiswal A, Prashanth K G and Manivasagam G 2021 A review on development of Bio-Inspired implants using 3D printing *Biomimetics* **6** 65
- [23] Maidin S, Abdullah A, Nor Hayati N M, Albaluoshi H and Alkahari R 2022 Application of taguchi method to optimize ultrasonic vibration assisted fused deposition modeling process parameters for surface roughness *J. Teknol.* **84** 125–33
- [24] Saba N, Jawaid M and Sultan M T H 2018 An overview of mechanical and physical testing of composite materials *Mechanical and Physical Testing of Biocomposites, Fibre-Reinforced Composites and Hybrid Composites* (Elsevier) 1–12
- [25] Li G, Zhao J, Wu W, Jiang J, Wang B, Jiang H and Fuh J 2018 Effect of ultrasonic vibration on mechanical properties of 3D printing Non-Crystalline and Semi-Crystalline polymers *Materials* **11** 826
- [26] Podroužek J, Marcon M, Ninčević K and Wan-Wendner R 2019 Bio-Inspired 3D infill patterns for additive manufacturing and structural applications *Materials* **12** 499